RSC Advances

ROYAL SOCIETY OF CHEMISTRY

www.rsc.org/advances

RSC Advances

Molybdenum disulfide nanoflakes through Li-AHA assisted exfoliation in aqueous medium

B.Bindhu,[*a] B.K. Sharu,[b] M.S. Gopika,[a] P.K. Praseetha[c] and K. Veluraja[d]

Two dimensional materials are the promising candidates for sensing, catalysis, and energy storage applications because of their high surface area and excellent electronic properties. Layered materials such as graphite, transition metal dichalcogenides (TMDs) and transition metal oxides (TMOs) can be the major source of two dimensional systems. However, the development of two dimensional systems from the layered materials has been hindered by the lack of proper exfoliation technique. We report the exfoliation of bulk MoS_2 powder into few layered nanoflakes using lithium salt of 6-aminohexanoic acid (Li-AHA) in aqueous dispersion. Li-AHA treated MoS_2 was 'destacked' to form few layered nanoflakes due to the electrostatic repulsion. XRD analysis showed that the Li-AHA treatment resulted in the formation of highly crystalline MoS_2 nanoflakes. Raman spectroscopic analysis indicated a shift in E^1_{2g} and A_{1g} peak suggesting the reduction in interlayer interaction, which in turn indicates the exfoliation. Electron microscopic observations strongly suggested the formation of few layered structure. These nanoflakes can be further incorporated into various polymer matrices to prepare composites with superior mechanical and electrical properties as compared to its bulk counterpart. The reported exfoliation technique is simple, effective and can be extended to exfoliate various transition metal dichalcogenides.

Introduction

Molybdenum disulfide (MoS_2), belonging to the family of layered transition metal dichalcogenides (TMDs), has been a subject of focused research in recent years due to its unusual structure and superior electrical, optical and mechanical properties. It is widely used as a solid lubricant[1,2] in aerospace, military and also automotive applications. These layered materials are an important source for catalysis, sensing and energy storage applications. But the development of such materials has been limited because of the lack of a suitable liquid exfoliation method.[3]

The layered structure of MoS_2 crystallizes in hexagonal arrangement which consists of covalently bonded Mo and S atoms that gives rise to triple S-Mo-S sandwich layers. Such layers are stacked together by weak van der Waals forces. Hence the intra-layer bonding in MoS_2 is very strong as compared to the inter-layer bonding. The naturally occurring mineral form, 2H-MoS_2 has two layers possessing hexagonal symmetry in its unit cell. Each stable configuration of S-Mo-S layer is called 1H -MoS_2 monolayer. The bulk MoS_2 unit cell belongs to space group P63/mmc and contains six atoms (two Mo and four S). The structure is uniquely determined by the hexagonal lattice constant a, the out-of-plane lattice constant c, and the internal displacement parameter z, whose experimental values were determined as, a = 3.16 Å, c = 12.58 Å, and z = 0.12.[4]

The recent discovery of graphene from graphite, a layered material, led to further exploration of 2D structures of layered materials. Such 2D materials are expected to be the forerunners in the future generation nanodevices owing to their exceptional carrier transport, ease of fabrication[5] and tunable properties. The first report on the synthesis of inorganic fullerene-like MoS_2 based on the sulfidization of MoS_3 films by passing a stream of H_2S at elevated temperature (850–1050 °C) were made by Tenne and co-workers.[6] Thereafter, various nanostructures of MoS_2 namely nanowires, nanotubes, nanorods, nanoflakes, nanoribbons, nanosheets, nanocrystals, nanofilms and nanofibers were fabricated.[5,7–16] Different techniques such as hydrothermal route, direct reaction method, solid state reaction, electrochemical method, scotch tape method, sulfidation, chemical vapour deposition and electrospinning method were adopted to produce MoS_2 nanostructures. Monolayer MoS_2 exhibit diverse electronic,[5,7] optical,[8,9] mechanical,[10,11] thermal,[12,13] and chemical properties,[14,15] fundamentally different from their bulk counterpart owing to quantum-mechanical confinement effect.[16]

In contrast to the zero-gap pristine graphene, the presence of a direct bandgap of 1.8 eV in monolayer MoS_2 allowed the

[a.] Department of Physics, Noorul Islam Centre for Higher Education, Kumaracoil-629180, Tamil Nadu, India. Email: bindhu.krishna80@gmail.com; Fax:04651-250266; Tel: 0986598942
[b.] School of Mechanical and Building Sciences, VIT University, Vellore-632014, Tamil Nadu, India.
[c.] Department of Nanotechnology, Noorul Islam Centre for Higher Education, Kumaracoil- 629180, Tamil Nadu, India.
[d.] School of Advanced Sciences, VIT University, Vellore-632014, Tamil Nadu, India.

fabrication of a room temperature current on/off transistor switch.[5] This led to the inter-band tunnel FETs with lower power consumption, one of the crucial requirement in integrated circuits. Apart from being a solid lubricant, the 2D layered MoS_2 has been explored in the oil refining industry as hydro-treating catalyst,[17] for reversible exchange of lithium in non-aqueous lithium batteries,[14,18] new generation transistors,[5] electrochemical hydrogen storage,[15,19] DNA hybridization detection,[20] biosystems,[21] photovoltaic solar cells,[22] as nanocomposites,[23,24] nanotribiology,[25] and also to achieve spintronic and valleytronic effect.[26] These results are intriguing, which realizes the 2D mono and multi layered MoS_2 as an appealing material in next generation devices.

Several techniques have been employed for the exfoliation of MoS_2 into a few layered nanoflakes-structure. The weak interlayer interaction and a large separation of 0.615 nm between MoS_2 layers enable the intercalation and easy diffusion of the Li ions without much change in the volume. It was envisaged that the exfoliation of MoS_2 into separate layers was obtained by the charge transfer to the MoS_2 layers after the insertion of lithium atoms between these layers followed by the hydration of the resulting $LiMoS_2$. However, the chemical exfoliation of MoS_2 through Li intercalation followed by ultra-sonication in aqueous medium results in significant deviation from the hexagonal structure.[27,28,29] Obtaining stable structures of few layer MoS_2 nanoflakes with beyond 10^5 atoms is a real challenge, because such layers scroll up to nanotubes and quasi spherical nanoparticle inorganic fullerene like nanoparticles.[30] Coleman et al. have used a number of common solvents to estimate their suitability for exfoliation of bulk TMDs through ultrasonication.[3] On analyzing the liquid exfoliated few layer MoS_2, it was found to possess hexagonal structure. MoS_2 nanosheets with controllable morphologies have been synthesized by mixed–solvothermal method. The organic solvents were adhered to the surface of MoS_2 and the different absorbing effect of the two mixed–solvents on MoS_2 surfaces resulted in the formation of different morphologies.[31] Mechanical exfoliation using scotch-tape has produced single layer MoS_2 which showed an excellent photo responsivity as compared to the graphene-based device.[32] Jian Zhen Ou et al. fabricated quasi 2D- MoS_2 nanoflakes from MoS_2 bulk powder using a grinding-assisted liquid phase exfoliation technique.[33] Recently Clark et al. reported green synthesis technique for MoS_2 nanoflakes using chenodeoxycholic acid as surfactant, which resulted in high yields.[34] The use of various surfactants in exfoliating MoS_2 has been extensively reported.[24,35–37] A scalable 2D spatial confinement technique has been developed for in situ synthesis of few layered and highly crystalline MoS_2 nanosheets anchored on 3D porous carbon nanosheet networks.[38]

Sodium salt of 6-aminohexanoic acid (Na-AHA) have been employed to improve the dispersion state of multiwalled carbon nanotubes in various polymer matrices.[39,40] Non-covalent modification of expanded graphite (EG) with lithium salt of 6-aminohexanoic acid (Li-AHA) led to the exfoliation of EG and formed a few layer 'graphene-like' structure.[41] Such non-covalent surface modification is of particular interest because it enhances the dispersibility and do not alter the inherent properties of the carbon nanostructures.[42] It is reported that Na-AHA molecules were adsorbed on carbon nanotubes surface and facilitate the "debundling" of nanotube agglomerates through electrostatic charge repulsion and steric stabilization.[39] These organic molecules based on 6-aminohexanoic acid facilitate the 'de-agglomeration' of carbon nanotubes and 'de-stacking' of EG through the electrostatic repulsive forces due to the formation of electrical double layer in aqueous dispersion.[39–41]

Owing to its hydrophobic nature, exfoliating MoS_2 in water is challenging. Alkali lignin assisted exfoliation is one of the first studies on liquid-phase exfoliation of MoS_2 based on aqueous media.[43] Nanofibrillated cellulose has been used to produce water-based dispersions of MoS_2.[44] In this work we report a new route to produce few layer MoS_2 nanosheets through Li-AHA assisted liquid phase exfoliation of bulk MoS_2 powder in aqueous medium. The role of Li-AHA modifier in exfoliating MoS_2, its interaction with MoS_2 surface and the mechanism of exfoliation are discussed. This route permits the synthesis of few layer MoS_2 from bulk crystalline MoS_2 and it was envisaged that specific interaction between Li^+ ions of the modifier and the d-electron clouds of MoS_2 would lead to significant debundling of the MoS_2 layers. Moreover, the proposed exfoliation technique does not require high temperature treatment or any organic solvents and hence is a green synthesis route. This method can be employed as an alternative route to exfoliate other TMDs.

Experimental details

Materials

Lithium hydroxide (LiOH) (Sigma Aldrich, purity: 98%), 6-amino hexanoic acid (AHA) (Sigma Aldrich, Mw= 132.18; purity: 98%) and commercially available Molybdenum disulfide powder (LOBA Chemie, purity: 98%) are the materials used in the present work.

Exfoliation of MoS_2

6-aminohexanoic acid was neutralized using Lithium hydroxide to obtain Li-AHA. MoS_2 was treated with 1:1 (wt/wt), 1:2 (wt/wt) and 1:4 (wt/wt) of Li-AHA in order to understand the influence of Li-AHA concentration on the extent of exfoliation. The amount of MoS_2 was kept constant and the percentage of Li-AHA was varied to achieve different modifier concentrations. Bulk MoS_2 powder was initially dispersed in distilled water by ultra-sonication (probe type ultrasonic processor DP120, frequency 50 kHz) for 10 min. The required amount of Li-AHA was dissolved in deionized water and the solution was then added to the MoS_2 dispersion and further ultra-sonicated for 30 min. Subsequently, the dispersion was continuously heated and stirred over a hot plate to obtain a dry mixture of Li-AHA treated MoS_2. Further, the treated MoS_2 was dried under vacuum at 75 °C overnight to remove traces of water. Also, bulk MoS_2 was sonicated in deionized water for

the same duration (hereafter denoted as untreated MoS_2) to identify whether ultra-sonication could cause any exfoliation even in the absence of Li-AHA.

Characterization

X-ray diffraction (XRD) studies were carried out on a Philips X-Pert Pro. The incident X-rays (λ=1.54 Å) from the Cu-target were monochromatized using a Ni filter. XRD patterns were recorded with a step scan with step size of 0.02 between 5° and 70° (2θ).

Raman spectroscopic analysis was done using a HR 800 micro-Raman (HORIBA Jobin Yovon, France) for bulk, untreated and Li-AHA treated MoS_2 in the scanning range of 250 to 500 cm^{-1} with an incident laser of excitation wavelength 514 nm.

Scanning electron microscopic (SEM) analysis was carried out using an FEG-SEM (JSM-7600F, Japan) with an accelerating voltage of 10 kV. To prepare the samples for SEM analysis, a small quantity of bulk/ Li-AHA treated MoS_2 was dispersed in de-ionised water and a drop was placed on Si wafer and was then dried. Silicon wafer containing the dried MoS_2 sheets was then gold sputtered to obtain the micrographs.

The transmission electron microscopic (TEM) analyses were carried out on a JEOL JEM-2100 F, Japan, field emission electron microscope. To prepare the samples for TEM investigation, MoS_2 powder was dispersed in de-ionised water, and a drop of the dispersion was placed on the TEM grid, after which it was dried. Selected area electron diffraction (SAED) analysis was used to determine the crystalline morphology associated with MoS_2 layer during TEM investigation.

Results and discussion

XRD analysis of bulk MoS_2 and Li-AHA treated MoS_2

The XRD pattern of bulk MoS_2 and various Li-AHA treated MoS_2 are shown in fig. 1. The characteristic peaks of (002), (100), (102), (103),(006), (105), (110) and (112) appearing at 2θ=14.5, 32.8, 36.1, 39.8, 44.3, 50.06, 58.4 and 60.5 confirms 2H-MoS_2 with lattice constants a = 3.1616Å and c = 12.2985Å (JCPDS 37-1492).[45] The (002) peak indicates the stacking of single layers, whereas the set of higher angle peaks could provide information about the crystallinity within the layers.[46] At reflection 2θ=14.5°, corresponding to (002) peak of untreated MoS_2, the d-spacing is calculated to be 0.615 nm and it matches with the reported value of 2H-MoS_2.[47] It is noticed that the intensity of (002) diffraction peak of the Li-AHA treated MoS_2 decreases as compared to the untreated and it indicates the de-stacking of MoS_2 layers. Furthermore, there is a marginal shift to lower angles for (002) peaks of Li-AHA treated with respect to that hexagonal 2H-MoS_2 phase (a maximum shift of ~1.5 % for 1:4 Li-AHA treated MoS_2). The shift in the (002) peaks to lower angles suggests the lattice expansion along the c-axis for the introduction of crystal defects or strains owing to curvature of the layers.[31,37] The

marginal shift signifies that the lattice distortion is minimal after the exfoliation and hence the structure is relaxed. The (002) peak shift and variation in intensity are illustrated as inset in fig 1. The decrease in (002) peak intensity suggests the reduction in thickness of bulk MoS_2 flakes.[48] The strong (103) peaks for the Li-AHA treated samples reveals the highly crystalline nature[18] and this implies that the inlayer crystallinity of Li-AHA treated MoS_2 is significantly improved. Hence, the XRD observations imply that the Li-AHA
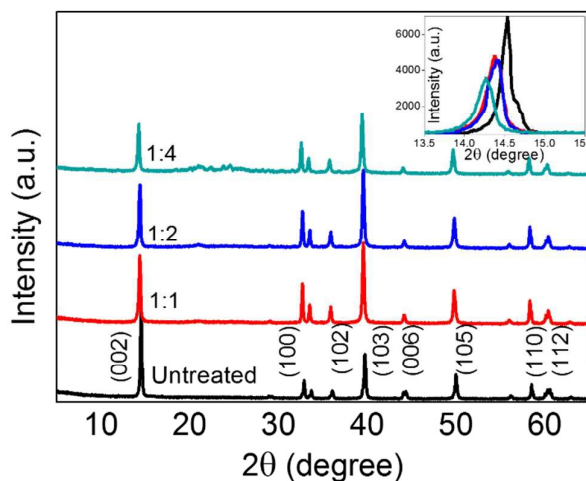
Fig. 1 XRD spectra of untreated and Li-AHA treated MoS_2

assisted liquid phase exfoliation is effectively de-stacking the bulk MoS_2 flakes.

Raman spectroscopic analysis of bulk, untreated and Li-AHA treated MoS_2

Raman spectroscopy is the most powerful non-destructive technique for the identification of 2D MoS_2 materials since the shift in prominent peak position and line width could provide information about the structure of the material. Fig. 2 shows the Raman spectra of bulk, untreated and Li-AHA treated MoS_2. The bulk MoS_2 shows two well defined peaks at 402 cm^{-1} and 376 cm^{-1} which are assigned to high energy A_{1g} and lower energy E^1_{2g} vibrational modes respectively,[49,50] and are separated by Δ=26 cm^{-1}. The E^1_{2g} mode signifies the in-layer displacements of Mo and S atoms and the A_{1g} mode represents the out-of-layer displacements of S atoms along the c-axis.[51] It is observed that there is no significant variation in peak values for the bulk and untreated MoS_2.

The spectra demonstrate that there is a significant blue shift in the E^1_{2g} and A_{1g} peaks of Li-AHA treated MoS_2 with respect to the bulk/untreated MoS_2. This observation is in direct contrast to most of the previous experimental studies on the MoS_2 material. Typically, in the exfoliated MoS_2 nanosheets the A_{1g} mode exhibits red-shift due to the deceased interlayer van der Waals force and the E^1_{2g} mode exhibits blue-shift due to the long-range Coulombic interlayer interactions.[52,53] However, the MoS_2 nanosheets produced by chemical-assisted exfoliation exhibited red-shift of E^1_{2g} mode and it was attributed to the adsorption of surfactants,

intercalation agents or solvents on the surface of the MoS_2 nanosheets.[43,54–56] Furthermore, the experimental studies on exfoliation of analogous WS_2 material showed a blue-shift of both the E_{2g} and A_{1g} peaks upon exfoliation to single layered material.[57]
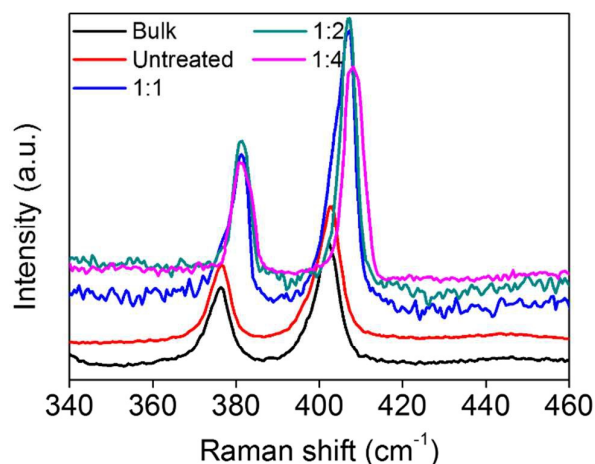
Fig. 2 Raman spectra of bulk, untreated, Li-AHA treated MoS_2

Change in the peak position could be investigated on the basis of resonance due to electronic and vibrational densities of state.[40] A considerable amount of blue shift (max. of ~ 6.2 cm^{-1}) is observed for the Li-AHA treated samples with respect to the bulk MoS_2. The reduction of the interlayer interaction for the exfoliated particles could lead to the observed shift to higher wave number at a constant laser excitation, indicating the "de-stacking" of MoS_2 layers. The vibrational densities of state may vary due to the adsorption of the Li-AHA molecules on MoS_2 surfaces, which may alter the vibrational modes of MoS_2. We believe that the surface modification of MoS_2 nanosheets by the adsorbed Li-AHA molecules could be the reason for the unusual blue shift of both the E^1_{2g} and A_{1g} peaks. Furthermore, the intensity of the peaks for Li-AHA treated MoS_2 are relatively higher and broader indicating the reduction in the thickness of bulk MoS_2 flakes.[55,57]

SEM analysis: Morphology of untreated and Li-AHA treated MoS_2

Fig. 3 shows the morphology of untreated and Li-AHA treated MoS_2. The SEM images give an insight into the exfoliation of untreated MoS_2 before and after Li-AHA intercalation. Fig. 3(a-c) clearly illustrates the multi layered structure of untreated MoS_2 and it is evident from the micrographs that the untreated MoS_2 exhibits a larger thickness. The SEM micrographs for 1:1 Li-AHA treated MoS_2 exhibits nanosheet morphology; a well dispersed and much thinner flakes could be seen Fig. 3(d-f). We attribute this effect to the exfoliation of MoS_2 in the presence of Li-AHA. Fig.3 (g-i) and fig. 3(j-l) shows the SEM images for 1:2 and 1:4 Li-AHA treated MoS_2. It is seen that many irregular layers of MoS_2 assemble to form floral structure for 1:2 Li-AHA treated MoS_2.

RSC Advances
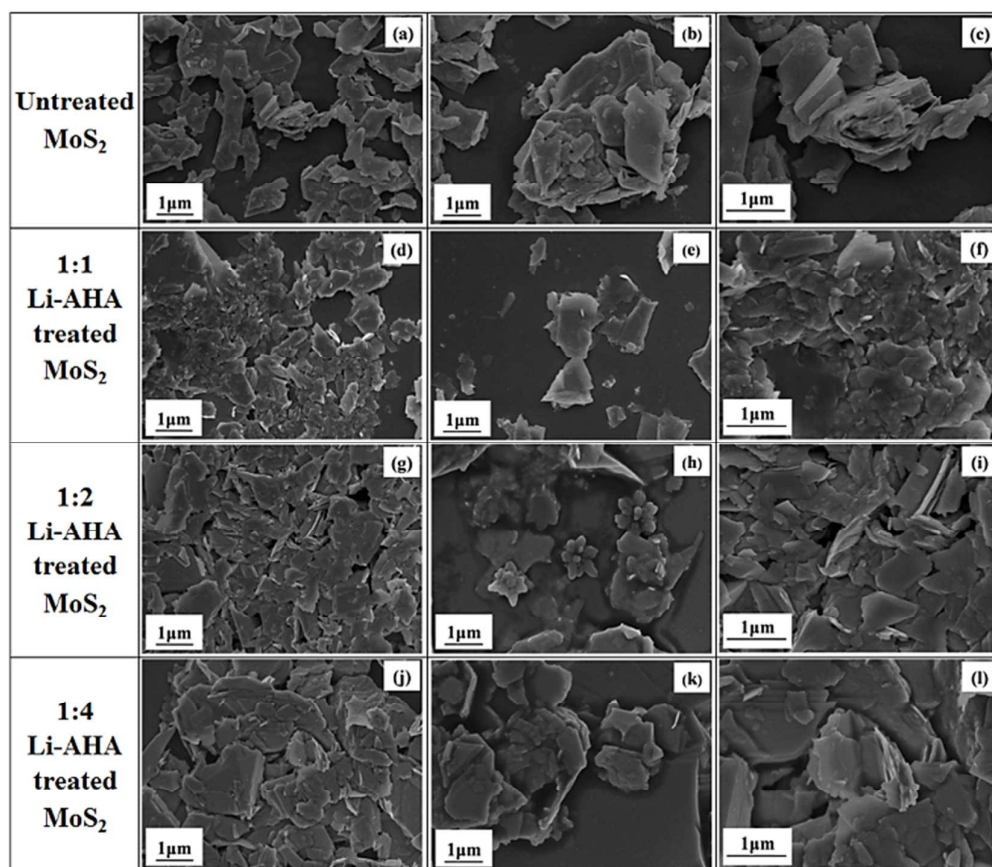
Fig. 3 SEM images of untreated and Li-AHA treated MoS_2 at 10000X, 15000X and 25000X magnifications: (a)-(c) untreated MoS_2; (d)-(f) 1:1 Li-AHA treated MoS_2; (g)-(i) 1:2 Li-AHA treated MoS_2; (j)-(l) 1:4 Li-AHA treated MoS_2

It is observed that the 'de-stacked' flakes forms clusters for higher Li-AHA concentration and also Li-AHA get adsorbed on the surface of MoS_2 nanosheets (fig. 3 (j-l)). The surface coverage of Li-AHA on MoS_2 nanoflakes could be advantageous as the aminemoiety on Li-AHA can act as a surface functionality and improves the interfacial interaction in various polymer matrices in case if this nanoflakes are further used to prepare polymer composites. The Li-AHA treatment led to the exfoliation of MoS_2 and forms the few layer nanoflakes. However, the Li-AHA concentration must be optimized to obtain an effective exfoliation.

TEM analysis - Morphology of untreated and Li-AHA treated MoS_2 & Identification of few layered structure using SAED

TEM and SAED analysis depicts the quantitative evidence for the exfoliation of untreated MoS_2 upon treating with Li-AHA. It is apparent from the TEM images that the Li-AHA treated MoS_2 has undergone an effective exfoliation and nanoflakes of a few layer MoS_2 are formed. It is observed that the nanosheets are slightly transparent to the electron beam, which indicates their ultrathin structure. Morphological investigation of untreated MoS_2 shows the layered 'platelet-like' structure with varying layer thickness and size for different platelets. The larger thickness of untreated MoS_2 flakes are evident from the SEM and TEM micrographs. The SAED analysis of untreated MoS_2 depicts a 'ring-like' pattern which indicate its 'polycrystalline' nature. On the other hand, all the Li-AHA treated samples exhibit 'hexagonal' dot pattern in the SAED analysis,

confirming the exfoliation of bulk MoS$_2$ into few layer nanosheets.
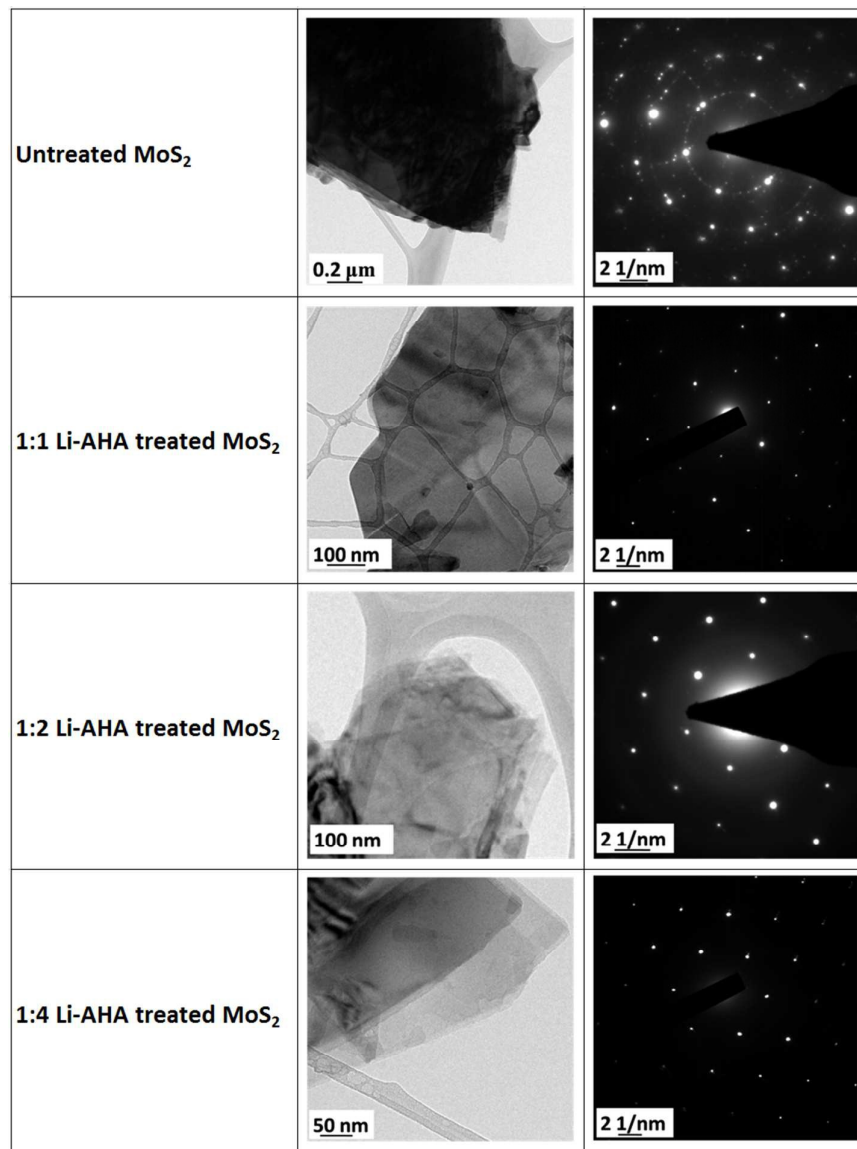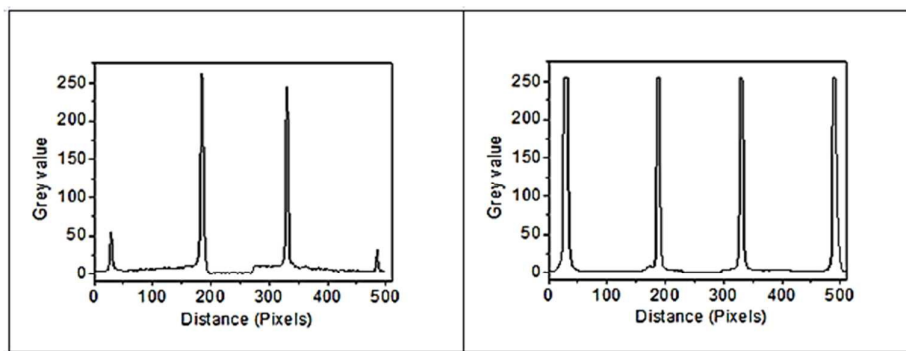
RSC Advances

PAPER

Furthermore, 1:1 Li-AHA concentration lead to the significant exfoliation as compared to the higher Li-AHA concentrations. The SAED pattern can also be used to distinguish between single and few layer MoS_2 by comparing the spot intensity profile of two adjacent planes in the hexagonal dot pattern. Single layer 2D material gives higher spot intensity for inner plane compared to outer plane, whereas a few-layer flake gives higher intensity for outer layer compared to inner layer.[58,59] Hence, the ratio of inner plane to outer plane spot intensity, I_R is greater than 1 for monolayer structure and less than 1 for a few layer structure. Fig. 5 illustrates the SAED analysis carried out for 1:1 and 1:4 Li-AHA treated MoS_2. It is seen that $I_R > 1$ for 1:1 Li-AHA content, which suggests the inner reflections are intense as compared to the outer reflection, confirming that the sample is consistent with isolated single layer structure. On the other hand, I_R is marginally less than 1 for 1:4 Li-AHA content, indicating a few layer structure of exfoliated MoS_2. Hence it is understood that exfoliation of MoS_2 with Li-AHA at appropriate concentration can yield monolayer flakes.

The MoS_2 platelets are stacked together by weak van der Waals forces and hence the inter-layer bonding is very weak as compared to the intra-layer covalent bonding in MoS_2. Li-AHA treated MoS_2 has been 'exfoliated' or 'destacked' to form a few layer nanoflakes due to the electrostatic repulsion, similar to the observation reported in the case of multiwalled carbon nanotubes and EG. Li-AHA on dissociation leads to Li^+ and AHA^- in deionized water. The weak interlayer interaction and large separation distance between the MoS_2 layers enable intercalation and easy diffusion of the Li^+ ions into the MoS_2 gallery. During ultra-sonication, the intercalated Li^+ ions could expedite the exfoliation of 'stacked' MoS_2 in the aqueous medium. Furthermore, the extended 'destacking' of MoS_2 platelets into a few layer nanoflakes in the presence of Li-AHA may be rationalized by the electrostatic charge repulsion between the negative charges due to the formation of an electrical double layer in aqueous dispersion. It could be explained in line with the exfoliation mechanisms postulated in case of debundling of nanotubes and exfoliation of EG.[39,41] The AHA^- could enter into the aggregates of MoS_2 stacks and break them up under ultra-sonication. Initially, the MoS_2 aggregates debundle due to the adsorption and intercalation of the modifier ions on the MoS_2 aggregates and gallery. Furthermore, these modifier molecules stabilize the dispersion through the electrostatic charge repulsion.

In aqueous solution, the MoS_2 surface is negatively charged due to the adsorbed AHA^- groups, whereas Li^+ ions may move throughout the aqueous medium and also intercalate in between the MoS_2 layers. The Li^+ ions may partly shield the negative charges on the MoS_2 surface and lead to the formation of an electrical double layer at MoS_2 surface with net negative charge. Subsequently, this leads to the stabilization of dispersed MoS_2 nanoflakes since the energy barrier for the 'restacking' of MoS_2 layers might be very high. Scheme 1 schematically illustrates the exfoliation mechanism of bulk MoS_2. Hence the exfoliation of bulk MoS_2 in to the few layer nanosheets can be envisaged as a synergistic effect of electrostatic repulsion due to the electrical double layer formation and the intercalation of Li^+ ions in to the MoS_2 gallery.
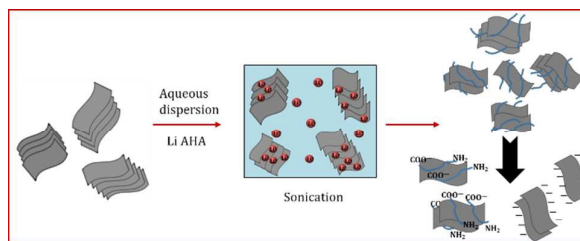
Scheme 1. Schematic showing the exfoliation mechanism of Li-AHA treated MoS_2 in deionized water

Conclusions

In brief, we have established that Li-AHA can be effectively used for the exfoliation of MoS_2. Three different Li-AHA concentrations have been tried to understand the influence of Li-AHA concentration on the extent of MoS_2 exfoliation. SEM and TEM analysis along with Raman Spectroscopic analysis and XRD indicated the exfoliation of MoS_2 into few layered nanoflakes. It was understood that well dispersed nanoflakes were obtained for 1:1 (wt/wt, MoS_2: Li-AHA) concentration. The reported exfoliation technique is simple and effective. Furthermore, we believe it is a general technique and can be extended to exfoliate various transition metal dichalcogenides and other layered materials.

Acknowledgements

References

1   M. H. Cho, J. Ju, S. J. Kim and H. Jang, *Wear*, 2006, **260**, 855–860.

2 X. Zhang, B. Luster, A. Church, C. Muratore, A. A. Voevodin, P. Kohli, S. Aouadi and S. Talapatra, *ACS Appl. Mater. Interfaces*, 2009, **1**, 735–739.

3 J. N. Coleman, M. Lotya, A. O'Neill, S. D. Bergin, P. J. King, U. Khan, K. Young, A. Gaucher, S. De, R. J. Smith, I. V Shvets, S. K. Arora, G. Stanton, H.-Y. Kim, K. Lee, G. T. Kim, G. S. Duesberg, T. Hallam, J. J. Boland, J. J. Wang, J. F. Donegan, J. C. Grunlan, G. Moriarty, A. Shmeliov, R. J. Nicholls, J. M. Perkins, E. M. Grieveson, K. Theuwissen, D. W. McComb, P. D. Nellist and V. Nicolosi, *Science*, 2011, **331**, 568–571.

4 Z. M. Wang, *Lecture Notes in Nanoscale Science and Technology. 2. Electronic structure of exfoliated MoS$_2$*, Springer International Publishing, Switzerland, 2010, 37-51.

5 B. Radisavljevic, A. Radenovic, J. Brivio, V. Giacometti and A Kis, *Nat. Nanotechnol.*, 2011, **6**, 147–150.

6 L. Margulis, G. Salitra, R. Tenne and M. Talianker, *Nature*, 1993, **365**, 113–114.

7 Q. H. Wang, K. Kalantar-Zadeh, A. Kis, J. N. Coleman and M. S. Strano, *Nat. Nanotechnol.*, 2012, **7**, 699–712.

8 G. Eda, H. Yamaguchi, D. Voiry, T. Fujita, M. Chen and M. Chhowalla, *Nano Lett.*, 2011, **11**, 5111–5116.

9 A. Splendiani, L. Sun, Y. Zhang, T. Li, J. Kim, C. Y. Chim, G. Galli and F. Wang, *Nano Lett.*, 2010, **10**, 1271–1275.

10 A. Kis, D. Mihailovic, M. Remskar, A. Mrzel, A. Jesih, I. Piwonski, A. J. Kulik, W. Benoît and L. Forró, *Adv. Mater.*, 2003, **15**, 733–736.

11 Q. Peng and S. De, *Phys. Chem. Chem. Phys.*, 2013, **15**, 19427–37.

12 L. F. Jie Su, Zheng-tang Liu, and N. Li, *J. Alloys Compd.*, 2015, **622**, 777–782.

13 T. H. Liu, Y. C. Chen, C. W. Pao and C. C. Chang, *Appl. Phys. Lett.*, 2014, **104**, 201909-1-201909-5.

14 R. Dominko, M. Gaberscek, D. Arcon, A. Mrzel, M. Remskar, D. Mihailovic, S. Pejovnik and J. Jamnik, *Electrochim. Acta*, 2003, **48**, 3079–3084.

15 J. Chen, S. L. Li, Q. Xu and K. Tanaka, *Chem. Commun.*, 2002, 1722–1723.

16 B. Radisavljevic and A. Kis, *Nat. Mater.*, 2013, **12**, 815–820.

17 M. Sun, J. Adjaye and A. E. Nelson, *Appl. Catal. A Gen.*, 2004, **263**, 131–143.

18 C. Feng, J. Ma, H. Li, R. Zeng, Z. Guo and H. Liu, *Mater. Res. Bull.*, 2009, **44**, 1811–1815.

19 J. Chen, N. Kuriyama, H. Yuan, H. T. Takeshita and T. Sakai, *J. Am. Chem. Soc.*, 2001, **123**, 11813–11814.

20 A. H. Loo, A. Bonanni, A. Ambrosi and M. Pumera, *Nanoscale*, 2014, **6**, 11971–11975.

21 J. Zhen Ou, A. F. Chrimes, Y. Wang, Shi-yang Tang, M. S. Strano and K. Kalantar-zadeh, *Nano Lett.*, 2014, **14**, 857–863.

22 M. Lin Tsai, S. H. Su, J. K. Chang, Dung-Sheng Tsai, Chang-Hsiao Chen, Chih-I Wu, Lain-Jong Li, Lih-Juann Chen and Jr-Hau He, *ACS Nano,* 2014, **8**, 8317-8322.

23 M. Naffakh, A. M. Díez-Pascual, M. Remškar and C. Marco, *J. Mater. Chem.*, 2012, **22**, 17002-17010.

24 K. Zhou, J. Liu, W. Zeng, Y. Hu and Z. Gui, *Compos. Sci. Technol.*, 2015, **107**, 120–128.

25 R. Rosentsveig, A. Gorodnev, N. Feuerstein, H. Friedman, a. Zak, N. Fleischer, J. Tannous, F. Dassenoy and R. Tenne, *Tribol. Lett.*, 2009, **36**, 175–182.

26 H. Zeng, J. Dai, W. Yao, D. Xiao and X. Cui, *Nat. Nanotechnol.*, 2012, **7**, 490–493.

27 G. L. Frey, K. J. Reynolds, R. H. Friend, H. Cohen and Y. Feldman, *J. Am. Chem. Soc.*, 2003, **125**, 5998–6007.

28 M. G. Kanatzidis, R. Bissessur, D. C. DeGroot, J. L. Schindler, C. R. Kannewurf, and C. Science, *Chem. Mater.*, 1993, **5**, 595–596.

29 R. A. Gordon, D. Yang, E. D. Crozier, D. T. Jiang and R. F. Frindt, *Phys. Rev. B*, 2002, **65**, 125407–1 – 9.

30 R. Tenne and G. Seifert, *Annu. Rev. Mater. Res.*, 2009, **39**, 387–413.

31 X. Feng, Q. Tang, J. Zhou, J. Fang, P. Ding, L. Sun and L. Shi, *Cryst. Res. Technol.*, 2013, **48**, 363–368.

32 Z. Yin, H. Li, H. Li, L. Jiang, Y. Shi, Y. Sun, G. Lu, Q. Zhang, X. Chen and H. Zhang, *ACS Nano*, 2012, **6**, 74–80.

33 E. P. Nguyen, B. J. Carey, T. Daeneke, J. Z. Ou, K. Latham, S. Zhuiykov and K. Kalantar-zadeh, *Chem. Mater.*, 2015, **27**, 53–59.

34 R. M. Clark, B. J. Carey, T. Daeneke, P. Atkin, M. Bhaskaran, K. Latham, I. S. Cole and K. Kalantar-zadeh, *Nanoscale*, 2015, **7**, 16763–16772.

35 G. Tang, Y. Wang, W. Chen, H. Tang and C. Li, *Mater. Lett.*, 2013, **100**, 15–18.

36 D. Wu, X. Zhou, X. Fu, H. Shi, D. Wang and Z. Hu, *J. Mater. Sci.*, 2006, **41**, 5682–5686.

37 Z. Wu, D. Wang and A. Sun, *J. Mater. Sci.*, 2010, **45**, 182–187.

38 J. Zhou, J. Qin, X. Zhang, C. Shi, E. Liu, J. Li, N. Zhao, C. He, M. Science, F. Materials and C. Science, *ACS Nano*, 2015, **9**, 3837–3848.

39 R. A. Khare, A. R. Bhattacharyya, A. S. Panwar, S. Bose and A. R. Kulkarni, *Polym. Eng. Sci.*, 2011, **51**, 1891–1905.

40 A. V Poyekar, A. R. Bhattacharyya, A. S. Panwar, G. P. Simon and D. S. Sutar, *ACS Appl. Mater. Interfaces*, 2014, **6**, 11054–11067.

41 M. S. Sreekanth, A. S. Panwar, P. Pötschke and A. R. Bhattacharyya, *Phys. Chem. Chem. Phys.*, 2015, **17**, 9410–9419.

42 N. G. Sahoo, S. Rana, J. W. Cho, L. Li and S. H. Chan, *Prog. Polym. Sci.*, 2010, **35**, 837–867.

43 W. Liu, C. Zhao, R. Zhou, D. Zhou, Z. Liu and X. Lu, *Nanoscale*, 2015, **7**, 9919–9926.

44 Y. Li, H. Zhu, F. Shen, J. Wan, S. Lacey, Z. Fang, H. Dai and L. Hu, *Nano Energy*, 2015, **13**, 346–354.

45 Y. Tian, Y. He and Y. Zhu, *Mater. Chem. Phys.*, 2004, **87**, 87–90.

46 P. Afanasiev, *Comptes Rendus Chim.*, 2008, **11**, 159–182.

47 M. Ahmad, M.A. Rafiq, Z. Imran, K. Rasool, R. N. Shahid, Y. Javed and M. M. Hasan, *J. Appl. Phys.*, 2013, **114**, 2011–2016.

48 V. H. Pham, K. H. Kim, D. W. Jung, K. Singh, E. S. Oh and J. S. Chung, *J. Power Sources*, 2013, **244**, 280–286.

49 L. Ma, G. Huang, W. Chen, Z. Wang, J. Ye, H. Li, D. Chen and J. Y. Lee, *J. Power Sources*, 2014, **264**, 262–271.

50 J. Kibsgaard, Z. Chen, B. N. Reinecke and T. F. Jaramillo, *Nat. Mater.*, 2012, **11**, 963–969.

51 T. Korn, S. Heydrich, M. Hirmer, J. Schmutzler and C. Schller, *Appl. Phys. Lett.*, 2011, **99**, 102109-1 - 102109-3

52 H. Li, Q. Zhang, C. Chong, R. Yap, K. Tay, T. Hang, T. Edwin, A. Olivier and D. Baillargeat, *Adv. Funct. Mater.*, 2012, **22**, 1385–1390.

53 C. Lee, H. Yan, L. E. Brus, T. F. Heinz, Ḱ. J. Hone and S. Ryu, *ACS Nano*, 2010, **4**, 2695–2700.

54 A. A. Jeffery, C. Nethravathi and M. Rajamathi, *J. Phys. Chem. C*, 2014, **118**, 1386–1396.

55 H. S. S. R. Matte, A. Gomathi, A. K. Manna, D. J. Late, R. Datta, S. K. Pati and C. N. R. Rao, *Angew. Chem. Int. Ed.*, 2010, **49**, 4059–4062.

56 W. Yin, L. Yan, J. Yu, G. Tian, L. Zhou, X. Zheng and X. Zhang, *ACS Nano*, 2014, **8**, 6922–6933.

57 S. M. Notley, *J. Colloid Interface Sci.*, 2013, **396**, 160–164.

58 Y. Hernandez, V. Nicolosi, M. Lotya, F. M. Blighe, Z. Sun, S. De, I. T. Mcgovern, B. Holland, M. Byrne, Y. K. Gunʹko, J. J. Boland, P. Niraj, G. Duesberg, S. Krishnamurthy, R. Goodhue, J. Hutchison, V. Scardaci, A. C. Ferrari and J. N. Coleman, N*at. Nanotechnol*. 2008, **3**, 563-568.

59 H. Tang, G. J. Ehlert, Y. Lin and H. A. Sodano, *Nano Lett.*, 2011, **12**, 84–90.

RSC Advances Accepted Manuscript

Graphical Abstract: **Manuscript Number: ID: RA-ART-11-2015-025368**

Title: **Molybdenum disulfide nanoflakes through Li-AHA assisted exfoliation in aqueous medium**
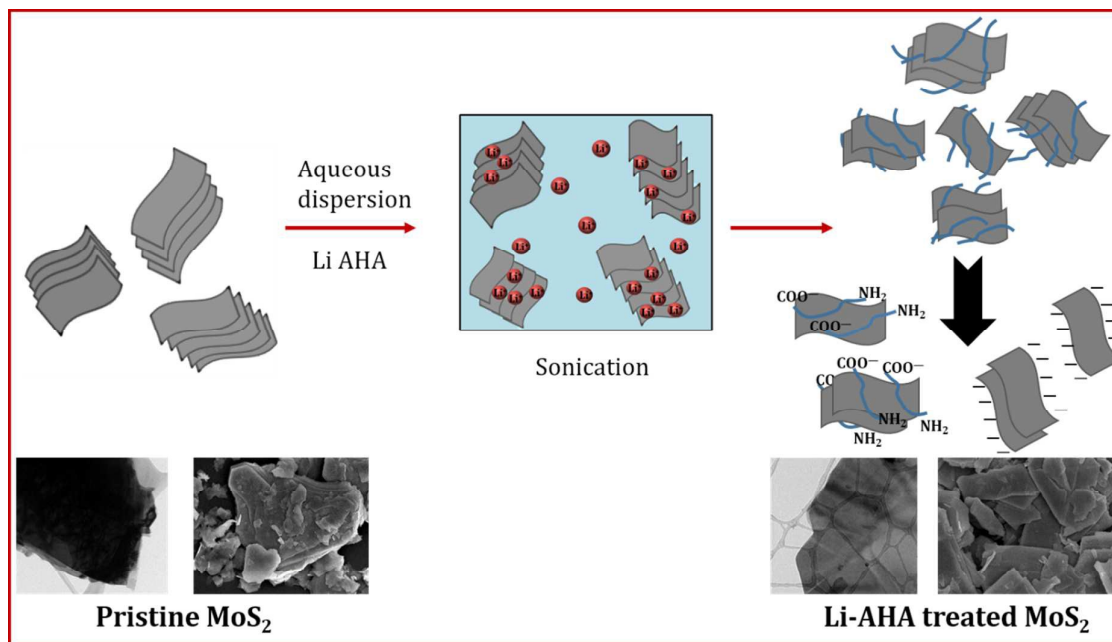
A novel route to synthesize MoS$_2$ nanoflakes though Li-AHA assisted liquid phase exfoliation